Random Growth Models

Patrik L. Ferrari*and Herbert Spohn†

3.3.2010

Abstract

The link between a particular class of growth processes and random matrices was established in the now famous 1999 article of Baik, Deift, and Johansson on the length of the longest increasing subsequence of a random permutation [BDJ99]. During the past ten years, this connection has been worked out in detail and led to an improved understanding of the large scale properties of one-dimensional growth models. The reader will find a commented list of references at the end. Our objective is to provide an introduction highlighting random matrices. From the outset it should be emphasized that this connection is fragile. Only certain aspects, and only for specific models, the growth process can be reexpressed in terms of partition functions also appearing in random matrix theory.

*Institute for Applied Mathematics, Bonn University, Endenicher Allee 60, 53115 Bonn, Germany; E-mail: ferrari@uni-bonn.de

†Department of Mathematics, Technical University of Munich, Boltzmannstr. 3, 85748 Garching, Germany; E-mail: spohn@ma.tum.de

1 Growth models

A growth model is a stochastic evolution for a height function $h(x,t)$, x space, t time. For the one-dimensional models considered here, either $x \in \mathbb{R}$ or $x \in \mathbb{Z}$. We first define the TASEP[1] (totally asymmetric simple exclusion process) with parallel updating, for which $h, x, t \in \mathbb{Z}$. An admissible height function, h, has to satisfy $h(x+1) - h(x) = \pm 1$. Given $h(x,t)$ and x_* a local minimum of $h(x,t)$, one defines

$$h(x_*, t+1) = \begin{cases} h(x_*,t) + 2 & \text{with probability } 1-q,\ 0 \le q \le 1\,, \\ h(x_*,t) & \text{with probability } q \end{cases} \tag{1}$$

independently for all local minima, and $h(x, t+1) = h(x,t)$ otherwise, see Figure 1 (left). Note that if $h(\cdot, t)$ is admissible, so is $h(\cdot, t+1)$.

There are two limiting cases of interest. At x_* the waiting time for an increase by 2 has the geometric distribution $(1-q)q^n$, $n = 0, 1, \ldots$. Taking the $q \to 1$ limit and setting the time unit to $1-q$ one obtains the exponential distribution of mean 1. This is the time-continuous TASEP for which, counting from the moment of the first appearance, the heights at local minima are increased independently by 2 after an exponentially distributed waiting time. Thus $h, x \in \mathbb{Z}$ and $t \in \mathbb{R}$.

The second case is the limit of rare events (Poisson points), where the unit of space and time is $\sqrt{q}$ and one takes $q \to 0$. Then the lattice spacing and time become continuous. This limit, after a slightly different height representation (see Section 5 for more insights), results in the polynuclear growth model (PNG) for which $h \in \mathbb{Z}$, $x, t \in \mathbb{R}$. An admissible height function is piecewise constant with jump size ± 1, where an increase by 1 is called an up-step and a decrease by 1 a down-step. The dynamics is constructed from a space-time Poisson process of intensity 2 of nucleation events. $h(x,t)$ evolves deterministically through (1) up-steps move to the left with velocity -1, down-steps move to the right with velocity $+1$, (2) steps disappear upon coalescence, and (3) at points of the space-time Poisson process the height is increased by 1, thereby nucleating an adjacent pair of up-step and down-step. They then move symmetrically apart by the mechanism described under (1), see Figure 1 (right).

The TASEP and PNG have to be supplemented by initial conditions and, possibly by boundary conditions. For the former one roughly divides between macroscopically flat and curved. For the TASEP examples would

[1]Here we use the height function representation. The standard particle representation consists in placing a particle at x if $h(x+1) - h(x) = -1$ and leaving empty if $h(x+1) - h(x) = 1$.

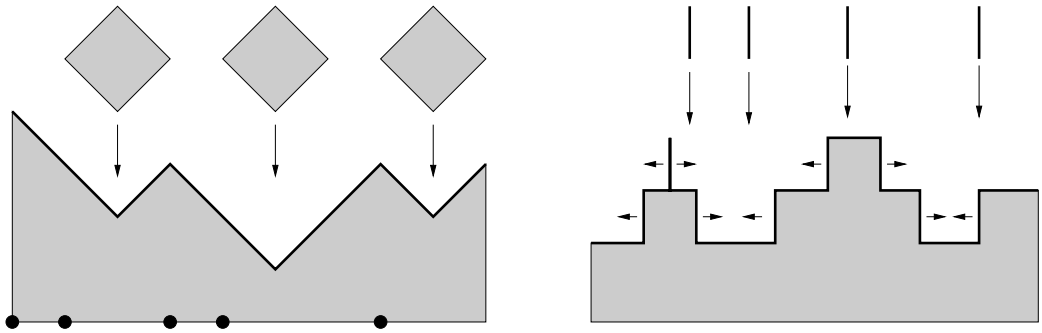

Figure 1: Growth of TASEP interface (left) and continuous time PNG (right)

be $h(x) = 0$ for x even and $h(x) = 1$ for x odd, which has slope zero, and $h(x+1) - h(x)$ independent Bernoulli random variables with mean m, $|m| \leq 1$, which has slope m. An example for a curved initial condition is $h(0) = 0$, $h(x+1) - h(x) = -1$ for $x = -1, -2, \ldots$, and $h(x+1) - h(x) = 1$ for $x = 0, 1, \ldots$.

What are the quantities of interest? The most basic one is the macroscopic shape, which corresponds to a law of large numbers for

$$\frac{1}{t} h\big([yt], [st]\big) \tag{2}$$

in the limit $t \to \infty$ with $y \in \mathbb{R}$, $s \in \mathbb{R}$, and $[\cdot]$ denoting integer part. From a statistical mechanics point of view the shape fluctuations are of prime concern. For example, in the flat case the surface stays macroscopically flat and advances with constant velocity v. One then would like to understand the large scale limit of the fluctuations $\{h(x,t) - vt, (x,t) \in \mathbb{Z} \times \mathbb{Z}\}$. As will be discussed below, the excitement is triggered through non-classical scaling exponents and non-Gaussian limits.

In 1986 in a seminal paper Kardar, Parisi, and Zhang (KPZ) proposed the stochastic evolution equation [KPZ86]

$$\frac{\partial}{\partial t} h(x,t) = \lambda \Big(\frac{\partial}{\partial x} h(x,t) \Big)^2 + \nu_0 \frac{\partial^2}{\partial x^2} h(x,t) + \eta(x,t) \tag{3}$$

for which $h, x, t \in \mathbb{R}$. $\eta(x,t)$ is space-time white noise which models the deposition mechanism in a moving frame of reference. The nonlinearity reflects the slope dependent growth velocity and the Laplacian with $\nu_0 > 0$ is a smoothing mechanism. To make the equation well-defined one has to introduce either a suitable spatial discretization or a noise covariance $\langle \eta(x,t)\eta(x',t') \rangle = g(x-x')\delta(t-t')$ with $g(x) = g(-x)$ and supported close

to 0. KPZ argue that, according to (3) with initial conditions $h(x,0) = 0$, the surface width increases as $t^{1/3}$, while lateral correlations increase as $t^{2/3}$. It is only through the connection to random matrix theory that universal probability distributions and scaling functions have become accessible.

Following TASEP, PNG, and KPZ as guiding examples it is easy to construct variations. For example, for the TASEP one could introduce evaporation through which heights at local maxima are decreased by 2. The deposition could be made to depend on neighboring heights. Also generalizations to higher dimensions, $x \in \mathbb{R}^d$ or $x \in \mathbb{Z}^d$, are easily accomplished. For the KPZ equation the nonlinearity then reads $\lambda\big(\nabla_x h(x,t)\big)^2$ and the smoothening is $\nu_0 \Delta h(x,t)$. For the PNG model in $d = 2$, at a nucleation event one generates on the existing layer a new layer of height one consisting of a disk expanding at unit speed. None of these models seem to be directly connected to random matrices.

2 How do random matrices appear?

Let us consider the PNG model with the initial condition $h(x,0) = 0$ under the constraint that there are no nucleations outside the interval $[-t,t]$, $t \geq 0$, which also refered to as PNG droplet, since the typical shape for large times is a semicircle. We study the probability distribution $\mathbb{P}(\{h(0,t) \leq n\})$, which depends only on the nucleation events in the quadrant $\{(x,s) |\, |x| \leq s, s-t \leq x \leq t-s\,,\ 0 \leq s \leq t\}$. Let us denote by $\omega = (\omega^{(1)}, \ldots, \omega^{(n)})$ a set of nucleation events and by $h(0,t;\omega)$ the corresponding height. The order of the coordinates of the $\omega^{(j)}$'s in the frame $\{x = \pm t\}$ naturally defines a permutation of n elements. It can be seen that $h(0,t;\omega)$ is simply the length of the longest increasing subsequence of that permutation. By the Poisson statistics of ω, the permutations are random and their length is Poisson distributed. By this reasoning, somewhat unexpectedly, one finds that $\mathbb{P}\big(\{h(0,t) \leq n\}\big)$ can be written as a matrix integral [BR01a]. Let $\mathcal{U}_n$ be the set of all unitaries on $\mathbb{C}^n$ and $\mathrm{d}U$ be the corresponding Haar measure. Then

$$\mathbb{P}\big(\{h(0,t) \leq n\}\big) = e^{-t^2} \int_{\mathcal{U}_n} \mathrm{d}U \exp[t \,\mathrm{tr}(U + U^*)]\,. \tag{4}$$

(4) can also be expressed as Fredholm determinant on $\ell_2 = \ell_2(\mathbb{Z})$. On ℓ_2 we define the linear operator B through

$$(Bf)(x) = -f(x+1) - f(x-1) + \frac{x}{t} f(x) \tag{5}$$

and denote by $P_{\leq 0}$ the spectral projection onto $B \leq 0$. Setting $\theta_n(x) = 1$ for $x > n$ and $\theta_n(x) = 0$ for $x \leq n$, one has

$$\mathbb{P}\big(\{h(0,t) \leq n\}\big) = \det(\mathbf{1} - \theta_n P_{\leq 0} \theta_n)\,. \tag{6}$$

Such an expression is familiar from GUE random matrices. Let $\lambda_1 < \ldots < \lambda_N$ be the eigenvalues of an $N \times N$ GUE distributed random matrix. Then

$$\mathbb{P}\big(\{\lambda_N \leq y\}\big) = \det(\mathbf{1} - \theta_y P_N \theta_y)\,. \tag{7}$$

Now the determinant is over $L^2(\mathbb{R}, \mathrm{d}y)$. If one sets $H = -\frac{1}{2}\frac{\mathrm{d}^2}{\mathrm{d}y^2} + \frac{1}{2N}y^2$, then P_N projects onto $H \leq \sqrt{N}$.

For large N one has the asymptotics

$$\lambda_N \cong 2N + N^{1/3}\xi_2 \tag{8}$$

with ξ_2 a Tracy-Widom distributed random variable, that is,

$$\mathbb{P}(\{\xi_2 \leq s\}) = F_2(s) := \det(\mathbf{1} - \chi_s K_{\mathrm{Ai}} \chi_s), \tag{9}$$

with det the Fredholm determinant on $L^2(\mathbb{R}, \mathrm{d}x)$, $\chi_s(x) = \mathbf{1}(x > s)$, and K_{Ai} is the Airy kernel (see (14) below). Hence it is not so surprising that for the height of the PNG model one obtains [PS00b]

$$h(0,t) = 2t + t^{1/3}\xi_2 \tag{10}$$

in the limit $t \to \infty$. In particular, the surface width increases as $t^{1/3}$ in accordance with the KPZ prediction. The law in (10) is expected to be universal and to hold whenever the macroscopic profile at the reference point, $x = 0$ in our example, is curved. Indeed for the PNG droplet $h(x,t) \cong 2t\sqrt{1-(x/t)^2}$ for large t, $|x| \leq t$.

One may wonder whether (10) should be regarded as an accident or whether there is a deeper reason. In the latter case, further height statistics might also be representable through matrix integrals.

3 Multi-matrix models and line ensembles

For curved initial data the link to random matrix theory can be understood from underlying line ensembles. They differ from case to case but have the property that the top line has the same statistics in the scaling limit. We first turn to random matrices by introducing matrix-valued diffusion processes.

Let $B(t)$ be GUE Brownian motion, to say $B(t)$ is an $N \times N$ hermitian matrix such that, for every $f \in \mathbb{C}^N$, $t \mapsto \langle f, B(t) f\rangle$ is standard Brownian

motion with variance $\langle f, f\rangle^2 \min(t, t')$ and such that for every unitary U it holds

$$UB(t)U^* = B(t) \tag{11}$$

in distribution. The $N \times N$ matrix-valued diffusion, $A(t)$, is defined through the stochastic differential equation

$$\mathrm{d}A(t) = -V'(A(t))\mathrm{d}t + \mathrm{d}B(t)\,, \quad A(0) = A, \tag{12}$$

with potential $V : \mathbb{R} \to \mathbb{R}$. We assume $A = A^*$, then also $A(t) = A(t)^*$ for all $t \geq 0$. It can be shown that eigenvalues of $A(t)$ do not cross with probability 1 and we order them as $\lambda_1(t) < \ldots < \lambda_N(t)$. $t \mapsto \big(\lambda_1(t), \ldots, \lambda_N(t)\big)$ is the line ensemble associated to (12).

In our context the largest eigenvalue, $\lambda_N(t)$ is of most interest. For $N \to \infty$ its statistics is expected to be independent of the choice of V. We first define the limit process, the Airy_2 process $\mathcal{A}_2(t)$, through its finite dimensional distributions. Let

$$H_{\mathrm{Ai}} = -\frac{\mathrm{d}^2}{\mathrm{d}y^2} + y \tag{13}$$

as a self-adjoint operator on $L^2(\mathbb{R}, \mathrm{d}y)$. The Airy operator has $\mathbb{R}$ as spectrum with the Airy function Ai as generalized eigenfunctions, $H_{\mathrm{Ai}}\mathrm{Ai}(y - \lambda) = \lambda \mathrm{Ai}(y - \lambda)$. In particular the projection onto $\{H_{\mathrm{Ai}} \leq 0\}$ is given by the Airy kernel

$$K_{\mathrm{Ai}}(y, y') = \int_0^\infty \mathrm{d}\lambda \mathrm{Ai}(y + \lambda)\mathrm{Ai}(y' + \lambda)\,. \tag{14}$$

The associated extended integral kernel is defined through

$$K_{\mathcal{A}_2}(y, \tau; y', \tau') = -(e^{-(\tau' - \tau)H_{\mathrm{Ai}}})(y, y')\mathbf{1}(\tau' > \tau) + (e^{\tau H_{\mathrm{Ai}}} K_{\mathrm{Ai}} e^{-\tau' H_{\mathrm{Ai}}})(y, y'). \tag{15}$$

Then, the m-th marginal for $\mathcal{A}_2(t)$ at times $t_1 < t_2 < \ldots < t_m$ is expressed as a determinant on $L^2(\mathbb{R} \times \{t_1, \ldots, t_m\})$ according to [PS02b]

$$\mathbb{P}\big(\mathcal{A}_2(t_1) \leq s_1, \ldots, \mathcal{A}_2(t_m) \leq s_m\big) = \det(\mathbf{1} - \chi_s K_{\mathcal{A}_2} \chi_s\big), \tag{16}$$

with $\chi_s(x, t_i) = \mathbf{1}(x > s_i)$. $t \mapsto \mathcal{A}_2(t)$ is a stationary process with continuous sample paths and covariance $g_2(t) = \mathrm{Cov}\big(\mathcal{A}_2(0), \mathcal{A}_2(t)\big) = \mathrm{Var}(\xi_2) - |t| + \mathcal{O}(t^2)$ for $t \to 0$ and $g_2(t) = t^{-2} + \mathcal{O}(t^{-4})$ for $|t| \to \infty$.

The scaling limit for $\mathcal{A}_2(t)$ can be most easily constructed by two slightly different procedures. The first one starts from the stationary Ornstein-Uhlenbeck process $A^{\mathrm{OU}}(t)$ in (12), which has the potential $V(x) = x^2/2N$.

Its distribution at a single time is GUE, to say $Z_N^{-1}\exp[-\frac{1}{2N}\mathrm{tr}A^2]\mathrm{d}A$, where the factor $1/N$ results from the condition that the eigenvalue density in the bulk is of order 1. Let $\lambda_N^{\mathrm{OU}}(t)$ be the largest eigenvalue of $A^{\mathrm{OU}}(t)$. Then

$$\lim_{N\to\infty} N^{-1/3}\big(\lambda_N^{\mathrm{OU}}(2N^{2/3}t) - 2N\big) = \mathcal{A}_2(t) \tag{17}$$

in the sense of convergence of finite dimensional distributions. The $N^{2/3}$ scaling means that locally $\lambda_N^{\mathrm{OU}}(t)$ looks like Brownian motion. On the other side the global behavior is confined.

The marginal of the stationary Ornstein-Uhlenbeck process for two time instants is the familiar 2-matrix model [EM98, NF98]. Setting $A_1 = A^{\mathrm{OU}}(0)$, $A_2 = A^{\mathrm{OU}}(t)$, $t > 0$, the joint distribution is given by

$$\frac{1}{Z_N^2}\exp\Big(-\frac{1}{2N(1-q^2)}\mathrm{tr}[A_1^2 + A_2^2 - 2qA_1A_2]\Big)\mathrm{d}A_1\mathrm{d}A_2, \quad q = \exp(-t/2N). \tag{18}$$

A somewhat different construction uses the Brownian bridge defined by (12) with $V = 0$ and $A^{\mathrm{BB}}(-T) = A^{\mathrm{BB}}(T) = 0$, that is

$$A^{\mathrm{BB}}(t) = B(T+t) - \frac{T+t}{2T}B(2T)\,, \quad |t| \le T\,. \tag{19}$$

The eigenvalues $t \mapsto \big(\lambda_1^{\mathrm{BB}}(t), \dots, \lambda_N^{\mathrm{BB}}(t)\big)$ is the Brownian bridge line ensemble. Its largest eigenvalue, $\lambda_N^{\mathrm{BB}}(t)$, has the scaling limit, for $T = 2N$,

$$\lim_{N\to\infty} N^{-1/3}\big(\lambda_N^{\mathrm{BB}}(2N^{2/3}t) - 2N\big) + t^2 = \mathcal{A}_2(t) \tag{20}$$

in the sense of finite-dimensional distributions. Note that $\lambda_N^{\mathrm{BB}}(t)$ is curved on the macroscopic scale resulting in the displacement by $-t^2$. But with this subtraction the limit is stationary.

To prove the limits (17) and (20) one uses in a central way that the underlying line ensemble are determinantal. For the Brownian bridge this can be seen by the following construction. We consider N independent standard Brownian bridges over $[-T, T]$, $b_j^{\mathrm{BB}}(t)$, $j = 1, \dots, N$, $b_j^{\mathrm{BB}}(\pm T) = 0$ and condition them on non-crossing for $|t| < T$. The resulting line ensemble has the same statistics as $\lambda_j^{\mathrm{BB}}(t)$, $|t| \le T$, $j = 1, \dots, N$, which hence is determinantal.

The TASEP, and its limits, have also an underlying line ensemble, which qualitatively resemble $\{\lambda_j^{\mathrm{BB}}(t),\, j = 1, \dots, N\}$. The construction of the line ensemble is not difficult, but somewhat hidden. Because of lack of space we explain only the line ensemble for the PNG droplet. As before t is the growth time and x is space which takes the role of t from above. The top

line is $\lambda_0(x,t) = h(x,t)$, h the PNG droplet of Section 1. Initially we add the extra lines $\lambda_j(x,0) = j$, $j = -1, -2, \ldots$. The motion of these lines is completely determined by $h(x,t)$ through the following simple rules: (1) and (2) from above are in force for all lines $\lambda_j(x,t)$, $j = 0, -1, \ldots$. (3) holds only for $\lambda_0(x,t) = h(x,t)$. (4) The annihilation of a pair of an adjacent down-step and up-step at line j is carried out and copied instantaneously as a nucleation event to line $j-1$.

We let the dynamics run up to time t. The line ensemble at time t is $\{\lambda_j(x,t), |x| \le t, j = 0, -1, \ldots\}$. Note that $\lambda_j(\pm t, t) = j$. Also, for a given realization of $h(x,t)$, there is an index j_0 such that for $j < j_0$ it holds $\lambda_j(x,t) = j$ for all $x, |x| \le t$. The crucial point of the construction is to have the statistics of the line ensemble determinantal, a property shared by the Brownian bridge over $[-t,t]$, $\lambda_j^{\mathrm{BB}}(x)$, $|x| \le t$. The multi-line PNG droplet allows for a construction similar to the Brownian bridge line ensemble. We consider a family of independent, rate 1, time-continuous, symmetric nearest neighbor random walks on $\mathbb{Z}$, $r_j(x)$, $j = 0, -1, \ldots$. The j-th random walk is conditioned on $r_j(\pm t) = j$ and the whole family is conditioned on non-crossing. The resulting line ensemble has the same statistics as the PNG line ensemble $\{\lambda_j(x,t), j = 0, -1, \ldots\}$, which hence is determinantal.

In the scaling limit for $x = \mathcal{O}(t^{2/3})$ the top line $\lambda_0(x,t)$ is displaced by $2t$ and $t^{1/3}$ away from $\lambda_{-1}(x,t)$. Similarly $\lambda_N^{\mathrm{BB}}(x)$ for $x = \mathcal{O}(N^{2/3})$ is displaced by $2N$ and order $N^{1/3}$ apart from $\lambda_{N-1}^{\mathrm{BB}}(x)$. On this scale the difference between random walk and Brownian motion disappears but the non-crossing constraint persists. Thus it is no longer a surprise that

$$\lim_{t\to\infty} t^{-1/3}\big(h(t^{2/3}x, t) - 2t\big) + x^2 = \mathcal{A}_2(x)\,, \quad x \in \mathbb{R}\,, \tag{21}$$

in the sense of finite dimensional distributions [PS02b].

To summarize: for curved initial data the spatial statistics for large t is identical to the family of largest eigenvalues in a GUE multi-matrix model.

4 Flat initial conditions

Given the unexpected connection between the PNG model and GUE multi-matrices, a natural question is whether such a correspondence holds also for other symmetry classes of random matrices. The answer is affirmative, but with unexpected twists. Consider the flat PNG model with $h(x,0) = 0$ and nucleation events in the whole upper half plane $\{(x,t), x \in \mathbb{R}, t \ge 0\}$. The removal of the spatial restriction of nucleation events leads to the problem of the longest increasing subsequence of a random permutation with involution [BR01b, PS00b]. The limit shape will be flat (straight) and in the limit

$t \to \infty$ one obtains

$$h(0,t) = 2t + \xi_1 t^{1/3}\,, \tag{22}$$

where

$$\mathbb{P}(\xi_1 \leq s) = F_1(2^{-2/3}s). \tag{23}$$

The distribution function F_1 is the Tracy-Widom distribution for the largest GOE eigenvalue.

As before, we can construct the line ensemble and ask if the link to Brownian motion on GOE matrices persists. Firstly, let us compare the line ensembles at fixed position for flat PNG and at fixed time for GOE Brownian motions. In the large time (resp. matrix dimension) limit, the edges of these point processes converge to the same object: a Pfaffian point process with 2×2 kernel [Fer04]. It seems then plausible to conjecture that also the two line ensembles have the same scaling limit, i.e., the surface process for flat PNG and for the largest eigenvalue of GOE Brownian motions should coincide. Since the covariance for the flat PNG has been computed exactly in the scaling limit, one can compare with simulation results from GOE multi-matrices. The evidence strongly disfavors the conjecture [BFP08].

The process describing the largest eigenvalue of GOE multi-matrices is still unknown, while the limit process of the flat PNG interface is known [BFS08] and called the Airy$_1$ process, $\mathcal{A}_1$,

$$\lim_{t\to\infty} t^{-1/3}\big(h(t^{2/3}x,t) - 2t\big) = 2^{1/3}\mathcal{A}_1(2^{-2/3}x). \tag{24}$$

Its m-point distribution is given in terms of a Fredholm determinant of the following kernel. Let $B(y,y') = \mathrm{Ai}(y+y')$, $H_1 = -\frac{\mathrm{d}}{\mathrm{d}y^2}$. Then,

$$K_{\mathcal{A}_1}(y,\tau;y',\tau') = -(e^{-(\tau'-\tau)H_1})(y,y')\mathbf{1}(\tau' > \tau) + (e^{\tau H_1}Be^{-\tau' H_1})(y,y') \tag{25}$$

and, as for the Airy$_2$ process, the m-th marginal for $\mathcal{A}_1(t)$ at times $t_1 < t_2 < \ldots < t_m$ is expressed through a determinant on $L^2(\mathbb{R}\times\{t_1,\ldots,t_m\})$ according to

$$\mathbb{P}\big(\mathcal{A}_1(t_1) \leq s_1, \ldots, \mathcal{A}_1(t_m) \leq s_m\big) = \det(\mathbf{1} - \chi_s K_{\mathcal{A}_1}\chi_s\big), \tag{26}$$

with $\chi_s(x,t_i) = \mathbf{1}(x > s_i)$ [Sas05, BFPS07]. The Airy$_1$ process is a stationary process with covariance $g_1(t) = \mathrm{Cov}\big(\mathcal{A}_1(0),\mathcal{A}_1(t)\big) = \mathrm{Var}(\xi_1) - |t| + \mathcal{O}(t^2)$ for $t \to 0$ and $g_1(t) \to 0$ super-exponentially fast as $|t| \to \infty$.

The Airy$_1$ process is obtained using an approach different from the PNG line ensemble, but still with an algebraic structure encountered also in random matrices (in the the GUE-minor process [JN06, OR06]). We explain the mathematical structure using the continuous time TASEP as model, since

the formulas are the simplest. For a while we use the standard TASEP representation in terms of particles. One starts with a formula by Schütz [Sch97] for the transition probability of the TASEP particles from generic positions. Consider the system of N particles with positions $x_1(t) > x_2(t) > \ldots > x_N(t)$ and let

$$G(x_1, \ldots, x_N; t) = \mathbb{P}(x_1(t) = x_1, \ldots, x_N(t) = x_N | x_1(0) = y_1, \ldots, x_N(0) = y_N). \tag{27}$$

Then

$$G(x_1, \ldots, x_N; t) = \det\left(F_{i-j}(x_{N+1-i} - y_{N+1-j}, t)\right)_{1 \le i,j \le N} \tag{28}$$

with

$$F_n(x,t) = \frac{1}{2\pi \mathrm{i}} \oint_{|w|>1} \mathrm{d}w \frac{e^{t(w-1)}}{w^{x-n+1}(w-1)^n}. \tag{29}$$

The function F_n satisfies the relation

$$F_n(x,t) = \sum_{y \ge x} F_{n-1}(y,t)\,. \tag{30}$$

The key observation is that (28) can be written as the marginal of a determinantal line ensemble, i.e. of a measure which is a product of determinants [Sas05]. The "lines" are denoted by x_i^n with time index n, $1 \le n \le N$, and space index i, $1 \le i \le n$. We set $x_1^n = x_n$. Then

$$G(x_1, \ldots, x_N; t) = \sum_{x_i^n, 2 \le i \le n \le N} \Big(\prod_{n=1}^{N-1} \det(\phi_n(x_i^n, x_j^{n+1}))_{i,j=1}^n \Big) \det(\Psi_{N-i}^N(x_j^N))_{i,j=1}^N \tag{31}$$

with $\Psi_{N-i}^N(x) = F_{-i+1}(x - y_{N+1-i}, t)$, $\phi_n(x,y) = \mathbf{1}(x > y)$ and $\phi_n(x_{n+1}^n, y) = 1$ (here x_{n+1}^n plays the role of a virtual variable). The line ensembles for the PNG droplet and GUE-valued Brownian motion have the same determinantal structure. However in (31) the determinants are of increasing sizes which requires to introduce the virtual variables x_{n+1}^n. However, from the algebraic perspective the two cases can be treated in a similar way. As a result, the measure in (31) is determinantal (for instance for any fixed initial conditions, but not only) and has a defining kernel dependent on $y_1, \ldots, y_N$. The distribution of the positions of TASEP particles are then given by a Fredholm determinant of the kernel. To have flat initial conditions, one sets $y_i = N - 2i$, takes first the $N \to \infty$ limit, and then analyzes the system in the large time limit to get the Airy_1 process defined above.

A couple of remarks:

(1) For general initial conditions (for instance for flat initial conditions), the

measure on $\{x_i^n\}$ is not positive, but some projections, like on the TASEP particles $\{x_1^n\}$, defines a probability measure.
(2) The method can be applied also to step initial conditions ($x_k(0) = -k$, $k = 1, 2, \ldots$) and one obtains the Airy$_2$ process. In this case, the measure on $\{x_i^n\}$ is a probability measure.
(3) In random matrices a measure which is the product of determinants of increasing size occurs too, for instance in the GUE-minor process [JN06, OR06].

5 Growth models and last passage percolation

For the KPZ equation we carry out the Cole-Hopf transformation $Z(x,t) = \exp(-\lambda h(x,t)/\nu_0)$ with the result

$$\frac{\partial}{\partial t} Z(x,t) = -\left(-\nu_0 \frac{\partial^2}{\partial x^2} + \frac{\lambda}{\nu_0}\eta(x,t)\right) Z(x,t)\,, \tag{32}$$

which is a diffusion equation with random potential. Using the Feynman-Kac formula, (32) corresponds to Brownian motion paths, x_t, with weight

$$\exp\left(-\frac{\lambda}{\nu_0}\int_0^t \mathrm{d}s\, \eta(x_s, s)\right). \tag{33}$$

In physics this problem is known as a directed polymer in a random potential, while in probability theory one uses directed first/last passage percolation. The spirit of the somewhat formal expression (33) persists for discrete growth processes. For example, for the PNG droplet we fix a realization, ω, of the nucleation events, which then determines the height $h(0,t;\omega)$ according to the PNG rules. We now draw a piecewise linear path with local slope m, $|m| < 1$, which starts at $(0,0)$, ends at $(0,t)$, and changes direction only at the points of ω. Let $L(t;\omega)$ be the maximal number of Poisson points collected when varying over allowed paths. Then $h(0,t;\omega) = L(t;\omega)$. So to speak, the random potential from (33) is spiked at the Poisson points.

In this section we explain the connection between growth models and (directed) last passage percolation. For simplicity, we first consider the case leading to discrete time PNG droplet, although directed percolation can be defined for general passage time distributions. Other geometries like flat growth are discussed later.

Let $\omega(i,j)$, $i,j \geq 1$, be independent random variables with geometric distribution of parameter q, i.e., $\mathbb{P}(\omega(i,j) = k) = (1-q)q^k$, $k \geq 0$. An up-right path π from $(1,1)$ to (n,m) is a sequence of points $(i_\ell, j_\ell)_{\ell=1}^{n+m-1}$ with

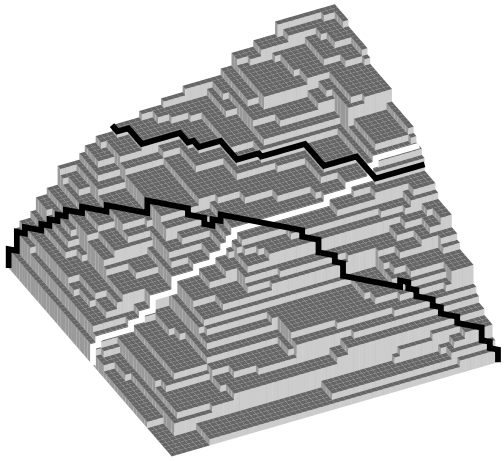

Figure 2: Directed percolation and growth models

$(i_{\ell+1}, j_{\ell+1}) - (i_\ell, j_\ell) \in \{(1,0),(0,1)\}$. The last passage time from $(1,1)$ to (n,m) is defined by

$$G(n,m) = \max_{\pi:(1,1)\to(n,m)} \sum_{(i,j)\in\pi} \omega(i,j). \tag{34}$$

The connection between directed percolation and different growth models is obtained by appropriate projections of the three-dimensional graph of G. Let us see how this works.

Let time t be defined by $t = i + j - 1$ and position by $x = i - j$. Then, the connection between the height function of the discrete time PNG and the last passage time G is simply [Joh03]

$$h(x,t) = G(i,j). \tag{35}$$

Thus, the discrete PNG droplet is nothing else than the time-slicing along the $i + j = t$ directions, see Figure 2.

We can however use also a different slicing, at constant $\tau = G$, to obtain the TASEP at time τ with step initial conditions. For simplicity, consider $\omega(i,j)$ to be exponentially distributed with mean one. Then $\omega(n,m)$ is the waiting time for particle m to do his nth jump. Hence, $G(n,m)$ is the time when particle m arrives at $-m+n$, i.e.,

$$\mathbb{P}(G(n,m) \le \tau) = \mathbb{P}(x_m(\tau) \ge -m + n). \tag{36}$$

From the point of view of the TASEP, there is another interesting cut, namely at fixed $j = n$. This corresponds to look at the evolution of the position of a given (tagged) particle, $x_n(\tau)$.

A few observations:
(1) Geometrically distributed random passage times correspond to discrete time TASEP with sequential update.
(2) The discrete time TASEP with parallel update is obtained by replacing $\omega(i,j)$ by $\omega(i,j)+1$.

The link between last passage percolation and growth holds also for general initial conditions. In (34) the optimization problem is called point-to-point, since both $(1,1)$ and (n,m) are fixed. We can generalize the model by allowing $\omega(i,j)$ to be defined on $(i,j) \in \mathbb{Z}^2$ and not only for $i,j \geq 1$. Consider the line $L = \{i+j=2\}$ and the following point-to-line maximization problem:

$$G_L(n,m) = \max_{\pi: L \to (n,m)} \sum_{(i,j)\in\pi} \omega(i,j). \tag{37}$$

Then, the relation to the discrete time PNG droplet, namely $h(x,t) = G_L(i,j)$ still holds but this time h is the height obtained from flat initial conditions. For the TASEP, it means to have at time $\tau = 0$ the particles occupying $2\mathbb{Z}$. Also random initial conditions fit in the picture, this time one has to optimize over end-points which are located on a random line.

In the appropriate scaling limit, for large time/particle number one obtains the Airy_2 (resp. the Airy_1) process for all these cases. One might wonder why the process seems not to depend on the chosen cut. In fact, this is not completely true. Indeed, consider for instance the PNG droplet and ask the question of joint correlations of $h(x,t)$ in space-time. We have seen that for large t the correlation length scales as $t^{2/3}$. However, along the rays leaving from $(x,t) = (0,0)$ the height function decorrelates on a much longer time scale, of order t. These slow decorrelation directions depend on the initial conditions. For instance, for flat PNG they are the parallel to the time axis. More generally, they coincide with the characteristics of the macroscopic surface evolution. Consequently, except along the slow directions, on the $t^{2/3}$ scale one will always see the Airy processes.

6 Growth models and random tiling

In the previous section we explained how different growth models (TASEP and PNG) and observables (TASEP at fixed time or tagged particle motion) can be viewed as different projections of a single three-dimensional object. A similar unifying approach exists also for some growth models and random tiling problems: there is a $2+1$ dimensional surface whose projection to one less dimension in space (resp. time) leads to growth in 1+1 dimensions (resp. random tiling in 2 dimensions) [BF08a]. To explain the idea, we consider the

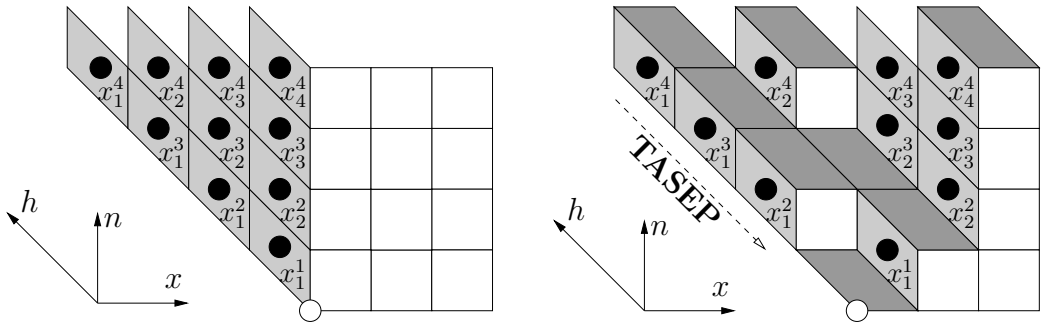

Figure 3: Illustration of the particle system and its corresponding lozenge tiling. The initial condition is on the left.

dynamical model connected to the continuous time TASEP with step initial conditions, being one of the simplest to define.

In Section 4 we encountered a measure on set of variables $S_N = \{x_i^n, 1 \le i \le n \le N\}$, see (31). The product of determinants of the ϕ_n's implies that the measure is non-zero, if the variables x_i^n belong to the set $S_N^{\rm int}$ defined through an interlacing condition,

$$S_N^{\rm int} = \{x_i^n \in S_N \,|\, x_i^{n+1} < x_i^n \le x_{i+1}^{n+1}\}. \tag{38}$$

Moreover, for TASEP with step initial conditions, the measure on $S_N^{\rm int}$ is a probability measure, so that we can interpret the variable x_i^n as the position of the particle indexed by (i, n). Also, the step initial condition, $x_n(t = 0) \equiv x_1^n(0) = -n$, implies that $x_i^n(0) = i - n - 1$, see Figure 3 (left).

Then, the dynamics of the TASEP induces a dynamics on the particles in $S_N^{\rm int}$ as follows. Particles independently try to jump on their right with rate one, but they might be blocked or pushed by others. When particle x_k^n attempts to jump:

(1) it jumps if $x_i^n < x_i^{n-1}$, otherwise it is blocked (the usual TASEP dynamics between particles with same lower index),

(2) if it jumps, it pushes by one all other particles with index $(i + \ell, n + \ell)$, $\ell \ge 1$, which are at the same position (so to remain in the set $S_N^{\rm int}$).

For example, consider the particles of Figure 3 (right). Then, if in this state of the system particle $(1, 3)$ tries to jump, it is blocked by the particle $(1, 2)$, while if particle $(2, 2)$ jumps, then also $(3, 3)$ and $(4, 4)$ will move by one unit at the same time.

It is clear that the projection of the particle system onto $\{x_1^n, 1 \le n \le N\}$ reduces to the TASEP dynamics in continuous time and step initial condi-

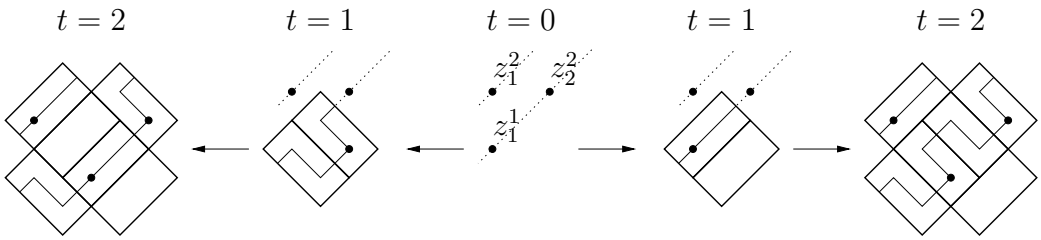

Figure 4: Two examples of configurations at time $t = 2$ obtained by the particle dynamics and its associated Aztec diamonds. The line ensembles are also drawn.

tions, this projection being the sum in (31).

The system of particles can also be represented as a tiling using three different lozenges as indicated in Figure 3. The initial condition corresponds to a perfectly ordered tiling and the dynamics on particles reflects a corresponding dynamics of the random tiling. Thus, the projection of the model to fixed time reduces to a random tiling problem. In the same spirit, the shuffling algorithm of the Aztec diamond falls into place. This time the interlacing is $S_{\text{Aztec}} = \{z_i^n \,|\, z_i^{n+1} \leq z_i^n \leq z_{i+1}^{n+1}\}$ and the dynamics is on discrete time, with particles with index n not allowed to move before time $t = n$. As before, particle (i, n) can be blocked by $(i, n-1)$. The pushing occurs in the following way: particle (i, n) is forced to move if it stays at the same position of $(i-1, n-1)$, i.e., if it would generate a violation due to the possible jump of particle $(i-1, n-1)$. Then at time t all particles which are not blocked or forced to move, jump independently with probability q. As explained in detail in [Nor08] this particle dynamics is equivalent to the shuffling algorithm of the Aztec diamond (take $q = 1/2$ for uniform weight). In Figure 4 we illustrate the rules with a small size example of two steps. There we also draw a set of lines, which come from a non-intersecting line ensemble similar to the ones of the PNG model and the matrix-valued Brownian motions described in Section 3.

On the other hand, let $x_i^n := z_i^n - n$. Then, the dynamics of the shuffling algorithm projected onto particles x_1^n, $n \geq 1$, is nothing else than the discrete time TASEP with parallel update and step initial condition! Once again, we have a $1+1$ dimensional growth and a 2 dimensional tiling model which are different projections of the same $2+1$-dimensional dynamical object.

7 A guide to the literature

There is a substantial body of literature and only a rather partial list is given here. The guideline is ordered according to physical model under study.

PNG model. A wide variety of growth processes, including PNG, are explained in [Mea98]. The direct link to the largest increasing subsequences of a random permutation and to the unitary matrix integral of [PS90] is noted in [PS00b, PS00a]. The convergence to the Airy_2 process is worked out in [PS02b] and the stationary case in [BR00, PS04]. For flat initial conditions, the height at a single space-point is studied in [BR01a, BR01b] and for the ensemble of top lines in [Fer04]. The extension to many space-points is accomplished by [BFS08]. Determinantal space-time processes for the discrete time PNG model are discussed by [Joh03]. External source at the origin is studied in [IS04b] for the full line and in [IS04a] for the half-line.

Asymmetric simple exclusion (ASEP). As a physical model reversible lattice gases, in particular the simple exclusion process, were introduced by Kawasaki [Kaw72] and its asymmetric version by Spitzer [Spi70]. We refer to Liggett [Lig99] for a comprehensive coverage from the probabilistic side. The hydrodynamic limit is treated in [Spo91] and [KL99], for example. There is a very substantial body on large deviations with Derrida as one of the driving forces, see [Der07] for a recent review. Schütz [Sch97] discovered a determinantal-like formula for the transition probability for a finite number of particles on $\mathbb{Z}$. TASEP step initial conditions are studied in the seminal paper by Johansson [Joh00]. The random matrix representation of [Joh00] may also be obtained by the Schütz formula [NS04, RS05]. The convergence to the Airy_2 process in a discrete time setting [Joh05]. General step initial conditions are covered by [PS02a] and the extended process in [BFP09]. In [FS06b] the scaling limit of the stationary two-point function is proved. Periodic intial conditions were first studied by Sasamoto [Sas05] and widely extended in [BFPS07]. A further approach comes from the Bethe ansatz which is used in [GS92] to determine the spectral gap of the generator. In a spectacular analytic tour de force Tracy and Widom develop the Bethe ansatz for the transition probability and thereby extend the Johansson result to the PASEP [TW09, TW08].

2D tiling (statics). The connection between growth and tiling was first understood in the context of the Aztec diamond [JPS98], who prove the arctic circle theorem. Because of the specific boundary conditions imposed, for typical tilings there is an ordered zone spatially coexisting with a

disordered zone. In the disordered zone the large scale statistics is expected to be governed by a massless Gaussian field, while the line separating the two zones has the Airy_2 process statistics.

a) Aztec diamond. The zone boundary is studied by [JPS98] and by [JN06]. Local dimer statistics are investigated in [CEP96]. Refined details are the large scale Gaussian statistics in the disordered zone [Ken00], the edge statistics [Joh05], and the statistics close to a point touching the boundary [JN06].

b) Ising corner. The Ising corner corresponds to a lozenge tiling under the constraint of a fixed volume below the thereby defined surface. The largest scale information is the macroscopic shape and large deviations [CK01]. The determinantal structure is noted in [OR03]. This can be used to study the edge statistics [FS03, FPS04]. More general boundary conditions (skew plane partitions) leads to a wide variety of macroscopic shapes [OR07].

c) Six-vertex model with domain wall boundary conditions, as introduced in [KZJ00]. The free energy including prefactors is available [BF06]. A numerical study can be found in [AR05]. The mapping to the Aztec diamond, on the free Fermion line, is explained in [FS06a].

d) Kasteleyn domino tilings. Kasteleyn [Kas63] noted that Pfaffian methods work for a general class of lattices. Macroscopic shapes are obtained by [KOS06] with surprising connections to algebraic geometry. Gaussian fluctuations are proved in [Ken08].

2D tiling (dynamics), see Section 6. The shuffling algorithm for the Aztec diamond is studied in [EKLP92, Pro03, Nor08]. The pushASEP is introduced by [BF08b] and anisotropic growth models are investigated in [BF08a], see also [PS97] for the Gates-Westcott model. A similar intertwining structure appears for Dyson's Brownian motions [War07].

Directed last passage percolation. "Directed" refers to the constraint of not being allowed to turn back in time. In the physics literature one speaks of a directed polymer in a random medium. Shape theorems are proved, e.g., in [Kes86]. While the issue of fluctuations had been repeatedly raised, sharp results had to wait for [Joh00] and [PS02b]. Growths models naturally lead to either point-to-point, point-to-line, and point-to-random-line last passage percolation. For certain models one has to further impose boundary conditions and/or symmetry conditions for the allowed domain. In (34) one takes the max, thus zero temperature. There are interesting results for the finite temperature version, where the energy appear in the exponential, as

in (33) [CY06].

KPZ equation. The seminal paper is [KPZ86], which generated a large body of theoretical work. An introductory exposition is [BS95]. The KPZ equation is a stochastic field theory with broken time reversal invariance, hence a great theoretical challenge, see, e.g., [Läs98].

Review articles. A beautiful review is [Joh06]. Growth models, of the type discussed here, are explained in [FP06,Fer08]. A fine introduction to random matrix techniques is [Sas07]. [KK08] provide an introductory exposition to the shape fluctuation proof of Johansson. The method of line ensembles is reviewed in [Spo06].

References

[AR05] D. Allison and N. Reshetikhin. Numerical study of the 6-vertex model with domain wall boundary conditions. *Ann. Inst. Fourier*, **55** (2005) 1847–1869.

[BDJ99] J. Baik, P.A. Deift, and K. Johansson. On the distribution of the length of the longest increasing subsequence of random permutations. J. Amer. Math. Soc., **12** (1999), 1119–1178.

[BFP09] J. Baik, P.L. Ferrari, and S. Péché. Limit process of stationary TASEP near the characteristic line. *arXiv:0907.0226* (2009).

[BF06] P. Bleher and V. Fokin. Exact solution of the six-vertex model with domain wall boundary condition, disordered phase. *Comm. Math. Phys.*, **268** (2006) 223–284.

[BF08a] A. Borodin and P.L. Ferrari. Anisotropic growth of random surfaces in $2 + 1$ dimensions. *arXiv:0804.3035* (2008).

[BF08b] A. Borodin and P.L. Ferrari. Large time asymptotics of growth models on space-like paths I: PushASEP. *Electron. J. Probab.*, **13** (2008) 1380-1418.

[BFP08] F. Bornemann, P.L. Ferrari, and M. Prähofer. The Airy_1 process is not the limit of the largest eigenvalue in GOE matrix diffusion. *J. Stat. Phys.*, **133** (2008) 405–415.

[BFPS07] A. Borodin, P.L. Ferrari, M. Prähofer, and T. Sasamoto. Fluctuation properties of the TASEP with periodic initial configuration. *J. Stat. Phys.*, **129** (2007) 1055–1080.

[BFS08] A. Borodin, P.L. Ferrari, and T. Sasamoto. Large time asymptotics of growth models on space-like paths II: PNG and parallel TASEP. *Comm. Math. Phys.*, **283** (2008) 417–449.

[BR00] J. Baik and E.M. Rains. Limiting distributions for a polynuclear growth model with external sources. *J. Stat. Phys.*, **100** (2000) 523–542.

[BR01a] J. Baik and E.M. Rains. Algebraic aspects of increasing subsequences. *Duke Math. J.*, **109** (2001) 1–65.

[BR01b] J. Baik and E.M. Rains. The asymptotics of monotone subsequences of involutions. *Duke Math. J.*, **109** (2001) 205–281.

[BS95] A.L. Barabási and H.E. Stanley. *Fractal Concepts in Surface Growth*. Cambridge University Press, Cambridge, 1995.

[CEP96] H. Cohn, N. Elkies, and J. Propp. Local statistics for random domino tilings of the Aztec diamond. *Duke Math. J.*, **85** (1996) 117–166.

[CK01] R. Cerf and R. Kenyon. The low-temperature expansion of the Wulff crystal in the 3D-Ising model. *Comm. Math. Phys*, **222** (2001) 147–179.

[CY06] F. Comets and N. Yoshida. Directed polymers in random environment are diffusive at weak disorder. *Ann. Probab.*, **34** (2006) 1746–1770.

[Der07] B. Derrida. Non-equilibrium steady states: fluctuations and large deviations of the density and of the current. *J. Stat. Mech.*, **P07023** (2007).

[EKLP92] N. Elkies, G. Kuperbert, M. Larsen, and J. Propp. Alternating-Sign Matrices and Domino Tilings I and II. *J. Algebr. Comb.*, **1** (1992) 111–132 and 219–234.

[EM98] B. Eynard and M.L. Mehta. Matrices coupled in a chain. I. Eigenvalue correlations. *J. Phys. A*, **31** (1998) 4449–4456.

[Fer04] P.L. Ferrari. Polynuclear growth on a flat substrate and edge scaling of GOE eigenvalues. *Comm. Math. Phys.*, **252** (2004) 77–109.

[Fer08] P.L. Ferrari. The universal Airy_1 and Airy_2 processes in the Totally Asymmetric Simple Exclusion Process. In J. Baik et al. editors, *Integrable Systems and Random Matrices: In Honor of Percy Deift*, Contemporary Math., pages 321–332. Amer. Math. Soc., 2008.

[FP06] P.L. Ferrari and M. Prähofer. One-dimensional stochastic growth and Gaussian ensembles of random matrices. *Markov Processes Relat. Fields*, **12** (2006) 203–234.

[FPS04] P.L. Ferrari, M. Prähofer, and H. Spohn. Fluctuations of an atomic ledge bordering a crystalline facet. *Phys. Rev. E*, **69** (2004) 035102(R).

[FS03] P.L. Ferrari and H. Spohn. Step fluctations for a faceted crystal. *J. Stat. Phys.*, **113** (2003) 1–46.

[FS06a] P.L. Ferrari and H. Spohn. Domino tilings and the six-vertex model at its free fermion point. *J. Phys. A: Math. Gen.*, **39** (2006) 10297–10306.

[FS06b] P.L. Ferrari and H. Spohn. Scaling limit for the space-time covariance of the stationary totally asymmetric simple exclusion process. *Comm. Math. Phys.*, **265** (2006) 1–44.

[GS92] L-H. Gwa and H. Spohn. The six-vertex model, roughened surfaces and an asymmetric spin Hamiltonian. *Phys. Rev. Lett.*, **68** (1992) 725–728 and *Phys. Rev. A*, **46** (1992) 844–854.

[IS04a] T. Imamura and T. Sasamoto. Fluctuations of the one-dimensional polynuclear growth model in a half space. *J. Stat. Phys.*, **115** (2004) 749–803.

[IS04b] T. Imamura and T. Sasamoto. Fluctuations of the one-dimensional polynuclear growth model with external sources. *Nucl. Phys. B*, **699** (2004) 503–544.

[JN06] K. Johansson and E. Nordenstam. Eigenvalues of GUE minors. *Electron. J. Probab.*, **11** (2006) 1342–1371.

[Joh00] K. Johansson. Shape fluctuations and random matrices. *Comm. Math. Phys.*, **209** (2000) 437–476.

[Joh03] K. Johansson. Discrete polynuclear growth and determinantal processes. *Comm. Math. Phys.*, **242** (2003) 277–329.

[Joh05] K. Johansson. The arctic circle boundary and the Airy process. *Ann. Probab.*, **33** (2005) 1–30.

[Joh06] K. Johansson. Random matrices and determinantal processes. In A. Bovier et al. editors, *Mathematical Statistical Physics, Session LXXXIII: Lecture Notes of the Les Houches Summer School 2005*, pages 1–56. Elsevier Science, 2006.

[JPS98] W. Jockush, J. Propp, and P. Shor. Random domino tilings and the arctic circle theorem. *arXiv:math.CO/9801068* (1998).

[Kas63] P.W. Kasteleyn. Dimer statistics and phase transitions. *J. Math. Phys.*, **4** (1963) 287–293.

[Kaw72] K. Kawasaki. Kinetics of Ising models. In C. Domb and M. S. Green, editors, *Phase Transitions and Critical Phenomena*. Academic Press, 1972.

[Ken00] R. Kenyon. The planar dimer model with boundary: a survey. *Directions in mathematical quasicrystals, CRM Monogr. Ser.*, **13** (2000) 307–328.

[Ken08] R. Kenyon. Height fluctuations in the honeycomb dimer model. *Comm. Math. Phys.*, **281** (2008) 675–709.

[Kes86] H. Kesten. Aspects of first-passage percolation. *Lecture Notes in Math.*, **1180** (1986) 125–264.

[KK08] T. Kriecherbauer and J. Krug. Interacting particle systems out of equilibrium. *arXiv:0803.2796* (2008).

[KL99] C. Kipnis and C. Landim. *Scaling Limits of Interacting Particle Systems*. Springer Verlag, Berlin, 1999.

[KOS06] R. Kenyon, A. Okounkov, and S. Sheffield. Dimers and amoebae. *Ann. of Math.*, **163** (2006) 1019–1056.

[KPZ86] K. Kardar, G. Parisi, and Y.Z. Zhang. Dynamic scaling of growing interfaces. *Phys. Rev. Lett.*, **56** (1986) 889–892.

[KZJ00] V. Korepin and P. Zinn-Justin. Thermodynamic limit of the six-vertex model with domain wall boundary conditions. *J. Phys. A*, **33** (2000) 7053–7066.

[Läs98] M. Lässig. On growth, disorder, and field theory. *J. Phys. C*, **10** (1998) 9905–9950.

[Lig99] T.M. Liggett. *Stochastic Interacting Systems: Contact, Voter and Exclusion Processes*. Springer Verlag, Berlin, 1999.

[Mea98] P. Meakin. *Fractals, Scaling and Growth Far From Equilibrium*. Cambridge University Press, Cambridge, 1998.

[NF98] T. Nagao and P.J. Forrester. Multilevel dynamical correlation functions for Dysons Brownian motion model of random matrices. *Phys. Lett. A*, **247** (1998) 42–46.

[Nor08] E. Nordenstam. On the shuffling algorithm for domino tilings. *Electron. J. Probab.*, **15** (2008) 75–95.

[NS04] T. Nagao and T. Sasamoto. Asymmetric simple exclusion process and modified random matrix ensembles. Nucl. Phys. B, **699** (2004) 487–502.

[OR03] A. Okounkov and N. Reshetikhin. Correlation function of Schur process with application to local geometry of a random 3-dimensional Young diagram. *J. Amer. Math. Soc.*, **16** (2003) 581–603.

[OR06] A. Okounkov and N. Reshetikhin. The birth of a random matrix. *Mosc. Math. J.*, **6** (2006) 553-566.

[OR07] A. Okounkov and N. Reshetikhin. Random skew plane partitions and the Pearcey process. *Comm. Math. Phys.*, **269** (2007) 571–609.

[Pro03] J. Propp. Generalized Domino-Shuffling. *Theoret. Comput. Sci.*, **303** (2003) 267–301.

[PS90] V. Perival and D. Shevitz. Unitary-matrix models as exactly solvable string theories. *Phys. Rev. Lett.*, **64** (1990) 1326–1329.

[PS97] M. Prähofer and H. Spohn. An Exactly Solved Model of Three Dimensional Surface Growth in the Anisotropic KPZ Regime. *J. Stat. Phys.*, **88** (1997) 999–1012.

[PS00a] M. Prähofer and H. Spohn. Statistical self-similarity of one-dimensional growth processes. *Physica A*, **279** (2000) 342–352.

[PS00b] M. Prähofer and H. Spohn. Universal distributions for growth processes in $1 + 1$ dimensions and random matrices. *Phys. Rev. Lett.*, **84** (2000) 4882–4885.

[PS02a] M. Prähofer and H. Spohn. Current fluctuations for the totally asymmetric simple exclusion process. In V. Sidoravicius, editor, *In and out of equilibrium*, Progress in Probability. Birkhäuser, 2002.

[PS02b] M. Prähofer and H. Spohn. Scale invariance of the PNG droplet and the Airy process. *J. Stat. Phys.*, **108** (2002) 1071–1106.

[PS04] M. Prähofer and H. Spohn. Exact scaling function for one-dimensional stationary KPZ growth. *J. Stat. Phys.*, **115** (2004) 255–279.

[RS05] A. Rákos and G. Schütz. Current Distribution and random matrix ensembles for an integrable asymmetric fragmentation process. *J. Stat. Phys.*, **118** (2005) 511–530.

[Sas05] T. Sasamoto. Spatial correlations of the 1D KPZ surface on a flat substrate. *J. Phys. A*, **38** (2005) L549–L556.

[Sas07] T. Sasamoto. Fluctuations of the one-dimensional asymmetric exclusion process using random matrix techniques. *J. Stat. Mech.*, **P07007** (2007).

[Sch97] G.M. Schütz. Exact solution of the master equation for the asymmetric exclusion process. *J. Stat. Phys.*, **88** (1997) 427–445.

[Spi70] F. Spitzer. Interaction of Markov processes. *Adv. Math.*, **5** (1970) 246–290.

[Spo91] H. Spohn. *Large Scale Dynamics of Interacting Particles*. Springer Verlag, Heidelberg, 1991.

[Spo06] H. Spohn. Exact solutions for KPZ-type growth processes, random matrices, and equilibrium shapes of crystals. *Physica A*, **369** (2006) 71–99.

[TW09] C.A. Tracy and H. Widom. Asymptotics in ASEP with step initial condition. *Comm. Math. Phys.*, **290** (2009) 129–154.

[TW08] C.A. Tracy and H. Widom. Integral Formulas for the Asymmetric Simple Exclusion Process. *Comm. Math. Phys.*, **279** (2008) 815–844.

[War07] Jon Warren. Dyson's Brownian motions, intertwining and interlacing. *Electron. J. Probab.*, **12** (2007) 573–590.